A collagen membrane containing osteogenic protein-1 promotes bone regeneration in a rat mandibular bone defect

Manami Ozaki

Nihon University Graduate School of Dentistry,

Major in Periodontology

(Directors: Prof. Shuichi Sato and Assist. Prof. Tadahiro Takayama)

Contents

The following article and new unpublished data (Fig. 4) are a part of this doctoral thesis:
A collagen membrane containing osteogenic protein-1 facilitates bone regeneration in a rat mandibular bone defect.
Manami Ozaki, Tadahiro Takayama, Takanobu Yamamoto, Yasumasa Ozawa, Mayu Nagao, Natsuko Tanabe, Akira Nakajima, Naoto Suzuki, Masao Maeno, Seiichi Yamano, Shuichi Sato

Archives of Oral Biology, Vol. 84, No. 8, (September, 2017) 19-28.

Abstract

Objectives: Osteogenic protein-1 (OP-1) exhibits osteoinductive activity and has applications in clinical treatment, including bone regeneration. Regenerative procedures using bioabsorbable collagen membranes (BCMs) have been well established in periodontal and implant dentistry. Here, the effects of OP-1 released from BCMs containing OP-1 (BCM/OP-1) on bone regeneration were evaluated *in vitro* and *in vivo*.

Design: For *in vitro* studies, cell viability and alkaline phosphatase activity were assessed after culture of MC3T3-E1 mouse pre-osteoblasts with BCM/OP-1. *In vivo* effects were investigated using a rat mandibular bone defect model. Eight rats underwent surgical operation of both sides of the mandible, and the 16 defects were divided into four groups: untreated control, BCM alone, BCM plus low-dose (0.5 μg) OP-1 (L-OP-1), and BCM plus high-dose (2.0 μg) OP-1 (H-OP-1). Newly formed bone was evaluated by micro-computed tomography (micro-CT) and histological analyses at 8 weeks after operation. The volume of new bone formation, bone density, and percentage of new bone area were evaluated.

Results: BCM/OP-1 had no cytotoxicity in MC3T3-E1 cells and increased alkaline phosphatase activity compared with control and BCM alone groups. BCM with OP-1 significantly increased bone volume, bone mineral density, and new bone area percentage in a dose-dependent manner compared with those of the control and BCM alone at 8 weeks after

surgical operation.

Conclusions: OP-1 delivered with BCMs may show osteoinduction and promote bone regeneration. The use of such a combination device for osteogenesis may result in safer and more predictable bone regenerative outcomes in the future.

Introduction

Bioresorbable collagen membranes (BCMs) have been widely used for guided bone regeneration (GBR), guided tissue regeneration (GTR) for periodontal regeneration, and improving bone defects for appropriate dental implant placement [1, 2]. Various synthetic and natural bioresorbable barriers have been prepared and studied *in vitro* and *in vivo* [3-6]. Collagen type I is a commonly used natural material, and polyglycolic acid is frequently used as a synthetic membrane that has potential applications in periodontal therapy [7]. Such materials must provide biocompatibility, tissue integration, cell occlusivity, and space-making ability for clinical applications [8]. Importantly, favorable results have been obtained for the use of BCM in dentistry and in various animal studies [9-11].

Collagen is a superior structural component involved in the formation of periodontal connective tissue and functions to activate coagulum formation and chemotaxis of periodontal ligament fibroblasts and gingival fibroblasts [12, 13]. Collagen is also a part of the extracellular matrix and serves as a fibrillar scaffold for vascular and tissue ingrowth [14]. Some synergistic approaches using BCMs and noncollagenous growth factors have been used to promote the regeneration of selective tissues. For example, bone morphogenetic proteins (BMPs), which belong to the transforming growth factor-β superfamily [15], are involved in tissue morphogenesis, regeneration, healing, and cell differentiation processes [16-18]. In particular,

BMPs have the ability to induce osteogenesis and are involved in embryonic development and fracture healing [19, 20].

Recombinant human (rh) BMP-2 and BMP-7 have been approved for clinical use in the regeneration of bone during fracture healing and spinal fusion [21, 22]. BMP-7, also called osteogenic protein-1 (OP-1), has been shown to have multiple biological activities in different cell types and strong anabolic activity in both bone and cartilage *in vitro* [23]. Previous studies have shown that the effects of OP-1 on cell proliferation are affected by cell type and culture conditions. Moreover, OP-1 stimulates both alkaline phosphatase (ALP) activity and osteocalcin production by osteoblast-like MC3T3-E1 cells in a concentration-dependent manner [24, 25]. OP-1 not only stimulates the maturation of committed osteoblast progenitors but also induces the commitment of undifferentiated nonosteogenic cells into osteoblasts [26].

Many *in vivo* studies have indicated the regenerative activity of OP-1, when biocompatible and/or biodegradable polymers are used with OP-1. Collagenous carriers and scaffolds as well as nanoparticles exhibit osteoinductive effects and can enhance fracture healing in rat femurs [27] and bone regeneration in mouse calvarial defects [28]. In clinical dentistry, hydroxyapatite (HA)-coated OP-1 promotes the healing of fresh dental extraction defects and enhances the osseointegration of dental implants with good initial stability. Application of OP-1 to bone defects increases the amount, density, and degree of bone

remodeling compared with untreated sites [29]. In addition, the use of OP-1 combined with a bovine collagen carrier has shown the the potential to induce bone formation in the human maxillary sinus after sinus floor elevation [30].

Recently, an *in vivo* study demonstrated that BCMs can successfully deliver sustained release of platelet-derived growth factor (PDGF) and that the delivered PDGF has osteogenic effects on rat mandibular defects [31]. Furthermore, BCMs containing growth/differentiation factor 5, which not only regulates cell growth and differentiation in both embryonic and adult tissues but also plays a role in skeletal development, significantly promotes bone regeneration compared with those of BCMs containing PDGF *in vivo* [32]. Moreover, BCMs containing stromal-derived factor-1 have been reported to have osteogenic effects on rat mandibular bone defects *in vivo* [33]. However, the effects of BCMs containing OP-1 (BCM/OP-1) on bone regeneration *in vivo* are not well understood.

Therefore, in this study, the effects of BCM/OP-1 on bone defects in the rat mandible were examined in order to improve clinical outcomes, such as healing speed and quantity and quality of newly formed bone, and to search for new candidates for bone regeneration.

Materials and Methods

Preparation of BCMs containing rhOP-1

A commercially available BCM, BioMend (crosslinked bovine type I collagen; Calcitek, Carlsbad, CA, USA), was prepared for *in vitro* or *in vivo* studies at sizes of 5 mm × 7.5 mm and 5 mm × 15 mm, respectively. rhOP-1 solution, carrier-free (R&D Systems, Minneapolis, MN, USA), was applied to the BCM. rhOP-1 was impregnated in the BCM just before the experiment. The amount of rhOP-1 applied to each BCM for each experiment was as follows: (1) enzyme-linked immunosorbent assay (ELISA): 0.5 or 2.0 μg rhOP-1, (2) 3-(4,5-dimethyl-thiazol-2yl)-2, 5-diphenyl tetrazolium bromide (MTT) assay: 50, 100, or 200 ng rhOP-1, (3) *in vivo* study: 0.5 μg (low concentration, L) or 2.0 μg (high concentration, H) rhOP-1.

ELISA for analysis of the release kinetics of rhOP-1 from BCM

The *in vitro* release kinetics of rhOP-1 from the BCM was determined over 2 weeks. *In vitro* release of rhOP-1 from the BCM was examined at 37°C in 2 mL phosphate-buffered saline (PBS). At predetermined intervals, the release medium was collected and replaced with fresh medium. Samples of 2 mL PBS containing rhOP-1 were collected at 1, 3, 5, 10, and 14 days and replaced with an equal amount of fresh PBS. Samples were stored at −20°C until

testing. All collected samples were centrifuged, filtered to remove free-floating impurities, and analyzed quantitatively using a Human OP-1 ELISA kit (R&D Systems) [34]. Data show the results of a single experiment (n = 3) that was repeated twice.

Cell culture

MC3T3-E1 murine calvaria pre-osteoblasts were obtained from Riken Bio Resource Center (Tsukuba, Japan) and cultured in α-minimal essential medium (α-MEM; Gibco BRL, Rockville, MD, USA) supplemented with 10% (v/v) fetal bovine serum HyClone Laboratories, Logan, UT, USA) and 1% (v/v) penicillin-streptomycin solution (Sigma-Aldrich, St. Louis, MO, USA) at 37°C in a humidified atmosphere of 95% air and 5% CO_2.

Effects of BCM/OP-1 on the viability of MC3T3-E1 cells

Cell viability was determined by reduction of MTT through NAD-dependent dehydrogenase activity. MC3T3-E1 cells (5×10^3 cells/well) in 80 μL of α-MEM supplemented with 10% FBS were seeded in clear-bottom 96-well tissue culture plates and incubated overnight. Subsequently, 15 μL MTT regent (Cell Viability Assay Kit; BioAssay Systems, Hayward, CA, USA) was added to each well, and the plates were incubated for 4 h at 37°C. After solutions were removed, dimethyl sulfoxide (100 μL/well) was added to

dissolve the formazan products, and the plates were shaken for 1 h at room temperature. The absorbance of each well was recorded on a microplate spectrophotometer at 570 nm to determine cell viability. The percentage of cell viability was calculated by comparing the appropriate optimal density with the control cells.

Effects of BCM/OP-1 on ALP activity in MC3T3-E1 cells

MC3T3-E1 cells (1×10^3 cells/well) were plated in 24-well plates and cultured. BCM containing rhOP-1 (50, 100, or 200 ng/mL) was added to the MC3T3-E1 cells, and the cells were then cultured for 7 days. Next, the cells were fixed with 4% paraformaldehyde for 10 min, washed twice with distilled water, and stained with ALP staining solution (pH 9.5, NBT/BCIP ready-to-use tablets; Roche Diagnostics GmbH, Penzberg, Germany).

Animals

In total, eight 10-week-old male Fischer 344jcl rats, weighing 220 ± 20 g each, were used. Animals were housed in pairs, in a specific pathogen-free environment, at a temperature of 22–23°C, relative humidity of 55%, and 12/12-h light/dark cycle. A standard commercial diet and tap water were available *ad libitum*. The study protocol was approved by the local

animal ethics committee in accordance with the Guidelines for Animal Experiments of Nihon University (AP14D035, AP16D031).

Evaluation of rat mandibular bone defects

Rats were anesthetized lightly by inhalation of isoflurane with O_2 and then subjected to deep general anesthesia by intraperitoneal (i.p.) injection of a mixture of 0.15 mg/kg dexmedetomidine hydrochloride, 2.0 mg/kg midazolam, and 2.5 mg/kg butorphanol tartrate. An i.p. injection of 500 μL of a 1:80,000 dilution of lidocaine (Xylocaine; Astra Zeneca, Osaka, Japan) was administered to control bleeding and provide additional anesthesia. The surgical areas were shaved, and the skin was washed with 70% ethanol before surgical incision. Under aseptic conditions, an incision was made through the masseter muscle, which was retracted to expose the bone around the mandibular angle, using a sterile no. 15 surgical blade (Feather Co., Osaka, Japan). Under nitrous-oxygen-isoflurane inhalation anesthesia, a full-thickness 4.0-mm circular critical-size defect was drilled into the mandibular angle with a trephine bur (Dentech, Tokyo, Japan), which was cooled intermittently by saline solution irrigation in a standardized surgical procedure. In the membrane-treated groups, the defects were covered with a barrier membrane, which was inserted between the bone and periosteum to secure around the mandibular angle and cover the defect completely (Fig. 1). The round

critical-sized (4.0 mm) defect in the rat mandibular angle did not heal naturally in controls at 24 weeks [35]. The muscle and skin layers were closed with 5-0 resorbable sutures (Alfresa Pharma Co., Osaka, Japan). The muscle and skin layers in control animals receiving "no treatment" were closed without covering the mandibular defect. Eight animals with bilateral defects (16 total defects) were used as the treatment group. A commercial softened food diet was provided for 7 days postoperation, followed by a normal food diet until the day of sacrifice. All rats were given 0.05 mg/kg buprenorphine by intramuscular injection for pain management for 3 days after surgery.

The mandibular defects were divided randomly into four experimental groups, as follows: group 1, no treatment control; group 2, BCM alone; group 3, BCM containing low-dose (0.5 μg) rhOP-1 (L-OP-1); and group 4, BCM containing high-dose (2.0 μg) rhOP-1 (H-OP-1). The rats were sacrificed at 8 weeks after surgery.

Evaluation of bone regeneration capability

Noninvasive assessments of *in vivo* bone regeneration were determined by micro-CT (R_mCT2 System; Rigaku, Tokyo, Japan) at the Nihon University School of Dentistry at 8 weeks postoperation. The CT settings used were as follows: pixel matrix, 480 × 480; voxel size, 30 × 30 × 30 μm; slice thickness, 120 μm; tube voltage, 90 kV; tube current, 100 μA;

and exposure time, 17 s. Three-dimensional (3D) isosurface rendering and images were constructed with the software provided by i-View (Kitasenjyu Radist Dental Clinic, i-View Image Center, Tokyo, Japan). Representative sections were cut from the vertical view after 3D reconstruction. Standard resolution mode was used to quantify the microstructural properties of the bone. A sagittal plane perpendicular to the central axis of the defect was determined, and the lateral and medial limits of the defect parallel to this plane were established. Every third two-dimensional micro-CT image between these limits was saved in a file. The amount of new bone formation within the defect region was assessed using micro-CT. The bone volume (BV) within the circular defects from voxel images was analyzed with BV measurement software (Kitasenjyu Radist Dental Clinic). A consistent volume of interest, located within the whole 4-mm-diameter region, was defined to evaluate the level of bone formation. The mineralized bone tissue was calculated using gray values and numbers of voxels with corresponding gray values in the regions of interest (ROIs). The BV fraction and bone mineral density were determined automatically and analyzed using built-in software. When unclosed defects were observed, ROIs were drawn around the respective boundaries on each image and interpolated to obtain volume renderings of the defects. The percentage of newly formed bone area in each of the measured areas was determined using Image J software (National Institutes of Health, Bethesda, MD, USA) [36].

Tissue processing and evaluation

At 8 weeks after the operation, all animals were euthanized using carbon dioxide (Raj et al., 2004). All sites of the mandible were examined radiographically using a dental X-ray unit (M-60; Softex, Japan) with an exposure time of 25 s (40 kV, 3 mA) and 12 × 16.5 cm X-ray film (IXFR; Fujifilm Co., Tokyo, Japan). Block biopsies including the defect surrounding soft tissue were collected. The mandibular ramus was explanted and fixed in 4% phosphate-buffered formalin solution. After 3 days of fixation, histopathological examinations were conducted on all mandibular defect sites. Samples were dissected and decalcified in K-CX (Falma, Tokyo, Japan) for 5 days and then neutralized in 5% sodium sulfate overnight. After cryoprotection in 20% sucrose in phosphate buffer, 12-μm frozen sections were prepared parallel to the sectioned surface and stained with hematoxylin and eosin (HE) for histological evaluation. Other specimens fixed with 70% ethanol were harvested and embedded in methyl methacrylate without decalcification after dehydration through a graded ethanol series, and Villanueva bone staining [38)] was then performed to evaluate pre-existing bone, new mineralized bone, and osteoids on 5-μm-thick sections of each specimen. Images were taken using a polarizing microscope (Eclipse LV100POL; Nikon Instech Co., Tokyo, Japan).

Statistical analyses

Each value represents the mean ± standard error (SEM). Statistical differences among the groups were assessed by one-way analysis of variance (ANOVA). Post hoc analyses using Tukey's test were performed to detect pairs of groups with statistical differences. All statistical analyses were performed using the GraphPad Prism 5 software (GraphPad Inc, La Jolla, CA). In all analyses, p values < 0.05 were considered to indicate statistical significance.

Results

rhOP-1 release from BCMs

Fig. 2 shows the kinetic release of rhOP-1 *in vitro*. BCMs containing rhOP-1 provided sustained release profiles of the two different effective doses (0.5 or 2.0 μg) from 1 to 14 days. In total, 0.42 ± 0.03 or 1.68 ± 0.01 μg was released continuously from the BCM at 14 days. Thus, ~85% of rhOP-1 was released cumulatively within 3 days, and the release rate was then decreased gradually until 14 days.

Cell viability of BCM carrying rhOP-1

MTT assays were performed to determine the viability of MC3T3-E1 cells cultured with BCM/OP-1. As shown in Fig. 3, the viabilities of cultured cells with BCM/OP-1 were similar to those of the negative control and BCM alone groups, indicating that the BCM/OP-1 complex was biocompatible. No apparent morphological changes in MC3T3-E1 cells were found in all culture conditions.

Effects of released rhOP-1 from BCM on cellular ALP

To evaluate the osteogenic effects of released rhOP-1 on MC3T3-E1 cells cultured with BCM/OP-1, ALP staining was performed (Fig. 4). BCM containing 200 ng OP-1 significantly

increased ALP staining intensity on MC3T3-E1 cells at 7 days compared with those of the control, BCM alone, and low-dose OP-1 groups.

Micro-CT evaluation of the effects of BCM/OP-1 on acceleration of bone formation

Representative micro-CT 3D images at 8 weeks demonstrated the effects of BCM/OP-1 on rat mandibular defects. The weights of the rats did not differ significantly between the conditions in each experimental period. H-OP-1 closed the defects completely with considerable lateral growth. Sagittal reconstruction of micro-CT images showed that the application of L-OP-1 filled the majority of sites with mineralized tissue. In contrast, BCM alone and control without OP-1 did not markedly close the defects (Fig. 5).

Morphometric results with micro-CT showed that BCM/OP-1 significantly increased the volume of new bone formation compared with BCM alone and the control at 8 weeks after surgery (Fig. 6A). The enhanced bone formation exhibited a dose-dependent response (H-OP-1 > L-OP-1). The density of new bone formation in the defect was also analyzed using micro-CT software (Fig. 6B). BCM/OP-1 complex significantly enhanced the new bone density compared with the control, and significant differences were found between BCM alone and H-OP-1 at 8 weeks after surgery. Analysis of the new bone ratio showed that BCM/OP-1 significantly enhanced new bone formation compared with BCM alone and the

control. Furthermore, the ratio in the H-OP-1 group was markedly greater than that in the L-OP-1 group (Fig. 6C).

Radiographic examination

X-ray images of representative specimens from the various groups are shown in Fig. 7. No radiopacity was observed at 8 weeks after surgery in the defects of the control and BCM alone groups. Mild radiopacities were detected within the defects. The BCM/OP-1 groups showed good induction of bone regeneration with lateral spreading at 8 weeks after surgery in the H-OP-1 group. Conspicuous radiopacities in L-OP-1 were observed with less bone formation inside the defects compared with that in H-OP-1.

Qualitative histological evaluation

Histological analysis of experimental groups (L-OP-1, H-OP-1) was performed to evaluate the osteogenic status of regenerated tissues within the defect sites. Microscopic examinations showed new bone formation originating from the bony borders of the defects towards the center. In contrast, in the control defects covered without a membrane, limited bone formation was observed. In the OP-1-treated defects, a dose-dependent increase in bone formation was found compared with those in the BCM alone and control groups, and new

bone completely filled the defects at 8 weeks after surgery. No adverse tissue reactions were observed. In the BCM/OP-1 groups, mature new bone was integrated with the host bone at marginal defects. Notably, in H-OP-1, mature new bone developed, and bone marrow cavity-like formation was observed in the marginal the defects. The mature new bone was thicker in the BCM/OP-1 group than in the BCM alone and control groups (Fig. 8).

To obtain evidence of the bone regenerative activity of BCM/OP-1, Villanueva bone staining, which was able to discriminate between mature bones (white staining) and fibrous tissues (blue staining), was performed. As shown in Fig. 9, in experimental models (L-OP-1 and H-OP-1), significant increases in new bone formation in mandibular defects were found on bony borders, similar to HE staining, at week 8.

In addition, thin sections of regenerated bone isolated from the OP-1-treated groups were assessed at 8 weeks after surgery. In both groups, osteoblasts, osteocytes, osteoids, and osteoclasts were found within the newly formed bone (Fig. 10).

Discussion

The use of animal models is often an essential step in the testing of new bone regeneration materials. Theoretically, experimental bone defects should be large enough to preclude spontaneous healing. The nonregenerative threshold of bone tissue has been investigated in various animal models. Critical-sized defects in animals are useful models for studying bone defects observed in the craniofacial skeleton. Critical-sized defects are defined as bony defects that will regenerate less than 10% of its prior bone stock over the lifetime of the animal [39]. Kaban et al. [40] reported that critical-size bone defects in the rat mandible must be more than 4 mm in diameter. These findings suggested that the appropriate size of mandibular defects is 4 mm in diameter to create critical-size bone defects. Das et al. [41] and Liu et al. [42] described a model using the rat mandibular bone as a suitable bone healing study for testing bone formation materials and substitutes until 8 weeks, since spontaneous healing was not complete in the created defects within 8 weeks. Additionally, moderate-to-severe degradation of the collagen membranes used here could be observed at 8 weeks for implantation [43]. Therefore, in this study, the 8-week time period was chosen as the final time point to induce mature healing of the defects. Indeed, bone regeneration was sufficient to fill the required bone volume in the defect at 8 weeks in the BCM/OP-1 group, particularly with H-OP-1.

Several studies have reported that combination of BMPs with scaffolds carriers and graft materials enhances bone healing [44-46]. Sawyer et al. [47] demonstrated that the release of rhBMP-2 from a collagen scaffold may be a clinically suitable approach for the repair and regeneration of critical-size craniofacial bone defects. Increasing the dose of rhBMP-7 has been shown to promote bone regeneration experimentally in furcation defects in beagle dogs[48]. These findings suggested that BMP-2 and -7 have similar effects on bone regeneration, and some minimal dose ranges are essential to increase bone regeneration beyond control levels.

Preliminary data indicated that OP-1 released from BCMs was detected during the first 3 days and that the levels were sustained until day 14, after which time, OP-1 was undetectable. This finding suggested that biphasic sustained release of OP-1 from BCM/OP-1 occurred during the early and later experimental times in which rapid or more gradual release of OP-1 was observed. The initial release of OP-1 has the advantage of "kick starting" osteoblasts in the bone defect, and delayed release of OP-1 is important for achieving adequate bone induction and mineralization [49]. Therefore, an effective delivery system may be required to release varying amounts of OP-1 spatially and temporally in order to optimize the growth of various components of the periodontium or bone tissues. The present study also supported that an appropriate dose of OP-1 released from the BCM enhanced *de novo* bone regeneration

and consolidation in circular rat mandibular bone defects.

ALP activity is an early phase osteoblastic marker to determine osteoblastic activity and differentiation [50]. The results showed that OP-1 released from BCM significantly increased ALP activity in MC3T3-E1 cells compared with those in the control and BCM alone groups. These data suggested that released OP-1 may affect the differentiation of MC3T3-E1 cells into osteoblasts.

The histological findings demonstrated an apparent natural healing process without inflammatory cells in all treatment groups, confirming the biocompatibility of the BCM/OP-1 complex. At 8 weeks after surgical operation, the defect site was replaced with newly formed bone. Micro-CT data at 8 weeks showed a high density of mineralized tissue in the defect area; some osteoblasts, osteoclasts, and osteocytes were observed in the bone-filled area on Villanueva-stained sections. Thus, native mandibular bone and newly formed bone at 8 weeks may have the same structural properties. Similar results have been described by Barr et al. [51] using OP-1 bioimplants (collagen membrane) in a mouse ectopic model. Berner et al. [52] used nanofibers containing OP-1 in the segmental defects of rat diaphyseal. Both studies demonstrated significantly higher BV in the OP-1 groups and supported the advantages of OP-1 in the treatment of critical-size defects.

In conclusion, these results showed that combination of OP-1 and BCM promoted

bone regeneration on rat mandibular bone defects. Moreover, BCM/OP-1 enhanced bone formation in a dose-dependent manner compared with those in the BCM alone and control groups after 8 weeks. Thus, OP-1 delivered with a BCM may have effective osteo-inducible potency and could be a good combination for bone regeneration. In addition, treatment with BCM/OP-1 in bone defects of the mandible induced regenerated BV and bone density, suggesting that OP-1 may have clinical applications in GTR or GBR. This is the first report demonstrating that BCM in combination with OP-1 may act as a stable osteoinductive complex and that traditional bone regeneration could be altered using BCM/OP-1. However, further studies using more animals and sequential experimental periods are needed to enable application of OP-1 in periodontal and implant dentistry. Additionally, in future investigations, the mechanisms of OP-1-mediated bone regeneration should be evaluated in association with the delivery system and the optimal conditions for OP-1 treatment in periodontal applications.

Conclusion

These results suggest that the BCMs containing OP-1 possessed osteoinductive properties that are sufficient to promote bone regeneration. The use of such a combination device for osteogenesis may result in safer and more predictable bone regenerative outcomes in the future.

Acknowledgements

The author thanks the Department of Biochemistry, Nihon University School of Dentistry, for technical advice and assistance and the Department of Pathology, Nihon University School of Dentistry, for histological imaging. The author also thanks Dr. Yoshinori Arai who assisted and commented on the micro-CT analysis. The author thanks the Ito Bone Histomorphometry Institute for analyzing histological sections of newly formed bone. This study was supported in part by a Grant-in-Aid for Young Scientists (B) (no. 15K20393 to T. Takayama) from the Ministry of Education, Culture, Sports, Science, and Technology (MEXT) of Japan and the Sato Fund, Nihon University School of Dentistry (to T. Takayama).

References

1. Sheikh, Z., Qureshi, J., Alshahrani, A. M., Nassar, H., Ikeda, Y., Glogauer, M., et al. (2017). Collagen based barrier membranes for periodontal guided bone regeneration applications. *Odontology*, 105, 1-12.
2. Stoecklin-Wasmer, C., Rutjes, A. W., da Costa, B. R., Salvi, G. E., Jüni, P., & Sculean, A. (2013). Absorbable collagen membranes for periodontal regeneration: a systematic review. *Journal of Dental Research*, 92, 773-781.
3. Bozkurt, A., Apel, C., Sellhaus, B., van Neerven, S., Wessing, B., Hilgers, R. D., et al. (2014). Differences in degradation behavior of two non-cross-linked collagen barrier membranes: an *in vitro* and *in vivo* study. *Clinical Oral Implants Research*, 25, 1403-1411.
4. Cui, J., Liang, J., Wen, Y., Sun, X., Li, T., Zhang, G., et al. (2014). *In vitro* and *in vivo* evaluation of chitosan/β-glycerol phosphate composite membrane for guided bone regeneration. *Journal of Biomedical Materials Research Part A*, 102, 2911-2917.
5. Hunter, K. T., & Ma, T. (2013). *In vitro* evaluation of hydroxyapatite-chitosan-gelatin composite membrane in guided tissue regeneration. *Journal of Biomedical Materials Research Part A*, 101, 1016-1025.

6. Sculean, A., Nikolidakis, D., & Schwarz, F. (2008). Regeneration of periodontal tissues: combinations of barrier membranes and grafting materials-biological foundation and preclinical evidence: a systematic review. *Journal of Clinical Periodontology*, 35, 106-116.

7. Berahim, Z., Moharamzadeh, K., Rawlinson, A., & Jowett, A. K. (2011). Biologic interaction of three-dimensional periodontal fibroblast spheroids with collagen-based and synthetic membranes. *Journal of Periodontology*, 82, 790-797.

8. Gottlow, J. (1993). Guided tissue regeneration using bioresorbable and non-resorbable devices: initial healing and long-term results. *Journal of Periodontology*, 64, 1157-1165.

9. Locci, P., Calvitti, M., Belcastro, S., Pugliese, M., Guerra, M., Marinucci, L., et al. (1997). Phenotype expression of gingival fibroblasts cultured on membranes used in guided tissue regeneration. *Journal of Periodontology*, 68, 857-863.

10. Mattson, J. S., Gallagher, S. J., & Jabro, M. H. (1999). The use of 2 bioabsorbable barrier membranes in the treatment of interproximal intrabony periodontal defects. *Journal of Periodontology*, 70, 510-517.

11. Oh, T. J., Meraw, S. J., Lee, E. J., Giannobile, W. V., & Wang, H. L. (2003). Comparative analysis of collagen membranes for the treatment of inplant dehiscence defects. *Clinical Oral Implants Research*, 14, 80-90.

12. Behring, J., Junker, R., Walboomers, X. F., Chessnut, B., & Jansen, J. A. (2008). Toward guided tissue and bone regeneration: morphology, attachment, proliferation, and migration of cells cultured on collagen barrier membranes. A systematic review. *Odontology*, 96, 1-11.

13. Piao, Z. G., Kim, J. S., Son, J. S., Lee, S. Y., Fang, X. H., Oh, J. S., et al. (2014). Osteogenic evaluation of collagen membrane containing drug-loaded polymeric microparticles in a rat calvarial defect model. *Tissue Engineering Part A*, 20, 3322-3331.

14. Patino, M. G., Neiders, M. E., Andreana, S., Noble, B., & Cohen, R. E. (2002). Collagen as an implantable material in medicine and dentistry. *Journal of Oral Implantology*, 28, 220-225.

15. Mikulski, A. J., & Urist, M. R. (1977). Collagenase-released non-collagenous proteins of cortical bone matrix. *Preparative Biochemistry*, 7, 357-381.

16. Al-Salleeh, F., Beatty, M. W., Reinhardt, R. A., Petro, T. M., & Crouch, L. (2008). Human osteogenic protein-1 induces osteogenic differentiation of adipose-derived stem cells harvested from mice. *Archives of Oral Biology*, 53, 928-936.

17. Koch, F. P., Becker, J., Terheyden, H., Capsius, B., & Wagner, W. (2010). A prospective, randomized pilot study on the safety and efficacy of recombinant human growth and

differentiation factor-5 coated onto β-tricalcium phosphate for sinus lift augmentation. *Clinical Oral Implants Research*, 21, 1301-1308.

18. Leknes, K. N., Yang, J., Qahash, M., Polimeni, G., Susin, C., & Wikesjö, U. M. (2008). Alveolar ridge augmentation using implants coated with recombinant human bone morphogenetic protein-7 (rhBMP-7/rhOP-1): radiographic observations. *Journal of Clinical Periodontology*, 35, 914-919.
19. Kroczek, A., Park, J., Birkholz, T., Neukam, F. W., Wiltfang, J., & Kessler, P. (2010). Effects of osteoinduction on bone regeneration in distraction: results of a pilot study. *Journal of Cranio-Maxillofacial Surgery*, 38, 334-344.
20. Zhong, W. J., Zhang, W. B., Ma, J. Q., Wang, H., Pan, Y. C., & Wang, L. (2011). Periostin-lile-factor-induced bone formation within orthopedic maxillary expansion. *Orthodontics & Craniofacial Research*, 14, 198-205.
21. Grauer, J. N., Vaccaro, A. R., Kato, M., Kwon, B. K., Beiner, J. M., Patel, T. C., et al. (2004). Development of a New Zealand white rabbit model of spinal pseudarthrosis repair and evaluation of the potential role of OP-1 to overcome pseudarthrosis. *Spine (Philadelphia, Pa. 1976)*, 29, 1405-1412.
22. Laursen, M., Høy, K., Hansen, E. S., Gelineck, J., Christensen, F. B., & Bünger, C. E. (1999). Recombinant bone morphogenetic protein-7 as an intracorporal bone growth

stimulator in unstable thoracolumbar burst fractures in humans: preliminary results. *European Spine Journal*, 8, 485-490.

23. Chubinskaya, S., & Kuettner, K. E. (2003). Regulation of osteogenic proteins by chondrocytes. *The International Journal of Biochemistry & Cell Biology*, 35, 1323-1340.
24. Asahina, I., Sampath, T. K., & Hauschka, P. V. (1996). Human osteogenic protein-1 induces chondroblastic, osteoblastic, and/or adipocytic differentiation of clonal murine target cells. *Experimental Cell Research*, 222, 38-47.
25. Zhang, F., Ren, L. F., Lin, H. S., Yin, M. N., Tong, Y. Q., & Shi, G. S. (2012). The optimal dose of recombinant human osteogenic protein-1 enhances differentiation of mouse osteoblast-like cells: an in vitro study. *Archives of Oral Biology*, 57, 460-468.
26. Tou, L., Quibria, N., & Alexander, J. M. (2003). Transcriptional regulation of the human Runx2/Cbfa1 gene promoter by bone morphogenetic protein-7. *Molecular and Cellular Endocrinology*, 205, 121-129.
27. Kidder, L. D., Chen, X., Schmidt, A. H., & Lew, W. D. (2009). Osteogenic protein-1 overcomes inhibition of fracture healing in the diabetic rat: a pilot study. *Clinical Orthopaedics and Related Research*, 467, 3249-3256.
28. Lee, Y. J., Lee, J. H., Cho, H. J., Kim, H. K., Yoon, T. R., & Shin, H. (2013). Electrospun fibers immobilized with bone forming peptide-1 derived from BMP7 for guided bone

regeneration. *Biomaterials*, 34, 5059-5069.

29. Cook, S. D., Salkeld, S. L., & Rueger, D. C. (1995). Evaluation of recombinant human osteogenic protein-1 (rhOP-1) placed with dental implants in fresh extraction sites. *Journal of Oral Implantology*, 21, 281-289.

30. Groenveld, H. H., Van den Bergh, J. P., Holzmann, P., Ten Bruggenkate, C. M., Tuinzing, D. B., & Burger, E. H. (1999). Histological observations of a bilateral maxillary sinus floor elevation 6 and 12 months after grafting with osteogenic protein-1 device. *Journal of Clinical Periodontology*, 26, 841-846.

31. Yamano, S., Lin, T. Y., Dai, J., Fabella, K., & Moursi, A. M. (2011). Bioactive collagen membrane as a carrier for sustained release of PDGF. *Journal of Tissue Science & Engineering*, 2, 110.

32. Yamano, S., Haku, K., Yamanaka, T., Dai, J., Takayama, T., Shohara, R., et al. (2014). The effect of a bioactive collagen membrane releasing PDGF or GDF-5 on bone regeneration. *Biomaterials*, 35, 2446-2453.

33. Takayama, T., Dai, J., Tachi, K., Shohara, R., Kasai, H., Imamura, K., et al. (2017). The potential of stromal-derived factor-1 delivery using a collagen membrane for bone regeneration. *Journal of Biomaterials Applications*, 31, 1049-1061.

34. Wang, H., Wu, G., Zhang, J., Zhou, K., Yin, B., Su, X., et al. (2016). Osteogenic effect of controlled released rhBMP-2 in 3D printed porous hydroxyapatite scaffold. *Colloids and Surfaces B: Biointerfaces*, 141, 491-498.

35. Kaban, L. B., Glowacki, J., & Murray, J. E. (1979). Repair of experimental mandibular bony defects in rats. *Surgical Forum*, 30, 519-521.

36. Sato, R., Matsuzaka, K., Kokubo, E., & Inoue, T. (2011). Immediate loading after implant placement following tooth extraction up-regulates cellular activity in the dog mandible. *Clinical Oral Implants Research*, 22, 1372-1378.

37. Raj, A. B., Leach, M. C., & Morton, D. B. (2004). Carbon dioxide for euthanasia of laboratory animals. *Comparative Medicine*, 54, 470-471.

38. Villanueva, A. R. (1974). A bone stain for osteoid seams in fresh, unembedded, mineralized bone. *Stain Technology*, 1, 1-8.

39. Hollinger, J. O., & Kleinschmidt, J. C. (1990). The critical size defect as an experimental model to test bone repair materials. *The Journal of Craniofacial Surgery*, 1, 60-68.

40. Kaban, L. B., Glowacki, J., & Murray, J. E. (1979). Repair of experimental mandibular bony defects in rats. *Surgical Forum*, 30, 519-521.

41. Das, A., Fishero, B. A., Christophel, J. J., Li, C. J., Kohli, N., Lin, Y., et al. (2016). Poly (lactic-co-glycolide) polymer constructs cross-linked with human BMP-6 and VEGF

protein significantly enhance rat mandible defect repair. *Cell and Tissue Research*, 364, 125-135.

42. Liu, H., Cui, J., Feng, W., Lv, S., Du, J., Sun, J., et al. (2015). Local administration of calcitriol positively influences bone remodeling and maturation during restoration of mandibular bone defects in rats. *Materials Science and Engineering: C Materials for Biological Applications*, 49, 14-24.
43. Owens, K. W., & Yukna, R. A. (2001). Collagen membrane resorption in dogs: a comparative study. *Implant Dentistry*, 10, 49-58.
44. Gautschi, O. P., Frey, S. P., & Zellweger, R. (2007). Bone morphogenetic proteins in clinical applications. *ANZ Journal of Surgery*, 77, 626-631.
45. Lind, M., Overgaard, S., Song, Y., Goodman, S. B., Bünger, C., & Søballe, K. (2000). Osteogenic protein 1 device stimulates bone healing to hydroxyapaptite-coated and titanium implants. *Journal of Arthroplasty*, 15, 339-346.
46. Ruhé, P. Q., Kroese-Deutman, H. C., Wolke, J. G., Spauwen, P. H., & Jansen, J. A. (2004). Bone inductive properties of rhBMP-2 loaded porous calcium phosphate cement implants in cranial defects in rabbits. *Biomaterials*, 25, 2123-2132.
47. Sawyer, A. A., Song, S. J., Susanto, E., Chuan, P., Lam, C. X., Woodruff, M. A., et al.

(2009). The stimulation of healing within a rat calvarial defect by mPCL-TCP/collagen scaffolds loaded with rhBMP-2. *Biomaterials*, 30, 2479-2488.

48. Giannobile, W. V., Ryan, S., Shih, M. S., Su, D. L., Kaplan, P. L., & Chan, T. C. (1998). Recombinant human osteogenic protein-1 (OP-1) stimulates periodontal wound healing in class III furcation defects. *Journal of Periodontology*, 69, 129-137.
49. Wei, G., Jin, Q., Giannobile, W. V., & Ma, P. X. (2007). The enhancement of osteogenesis by nano-fibrous scaffolds incorporating rhBMP-7 nanospheres. *Biomaterials*, 28, 2087-2096.
50. Huang, W., Yang, S., Shao, J., & Li, Y. P. (2007). Signaling and transcriptional regulation in osteoblast commitment and differentiation. *Frontiers in bioscience*, 12, 3068-3092.
51. Barr, T., Mcnamara, A. J., Sándor, G. K., Cokie, C. M., & Peel, S. A. (2010). Comparison of the osteoinductivity of bioimplants containing recombinant human bone morphogenetic proteins 2 (Infuse) and 7 (OP-1). *Oral Surgery, Oral Medicine, Oral Pathology, Oral Radiology, and Endodontology*, 109, 531-540.
52. Berner, A., Boerckel, J. D., Saifzadeh, S., Steck, R., Ren, J., Vaquette, C., et al. (2012). Biomimetic tubular nanofiber mesh and platelet rich plasma-mediated delivery of BMP-7 for large bone defect regeneration. *Cell and Tissue Research*, 347, 603-612.

Figures

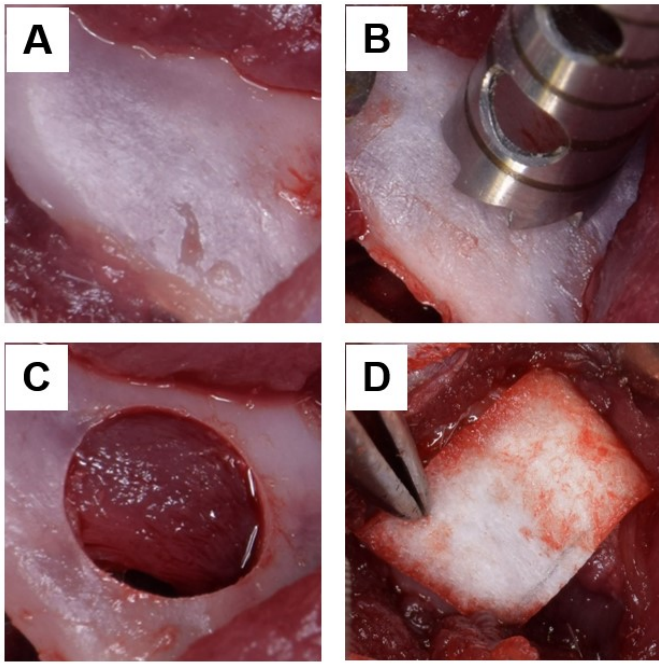

Fig. 1. Optical photos of the *in vivo* study using the rat mandibular bone defect model. Critical-size full-thickness defects measuring 4 mm in diameter were created on both sides of the mandibular ramus using a trephine bur (A–C). The BCM was stabilized around the mandibular angle and covered the defects completely (D).

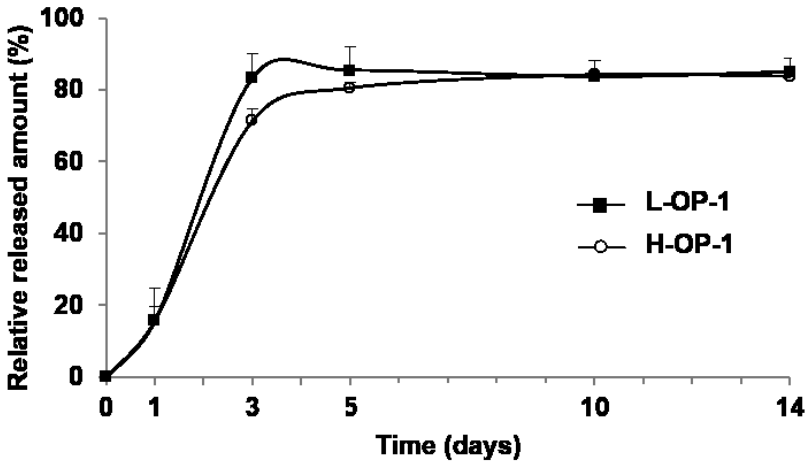

Fig. 2. The amount of rhOP-1 released from BCMs containing rhOP-1.

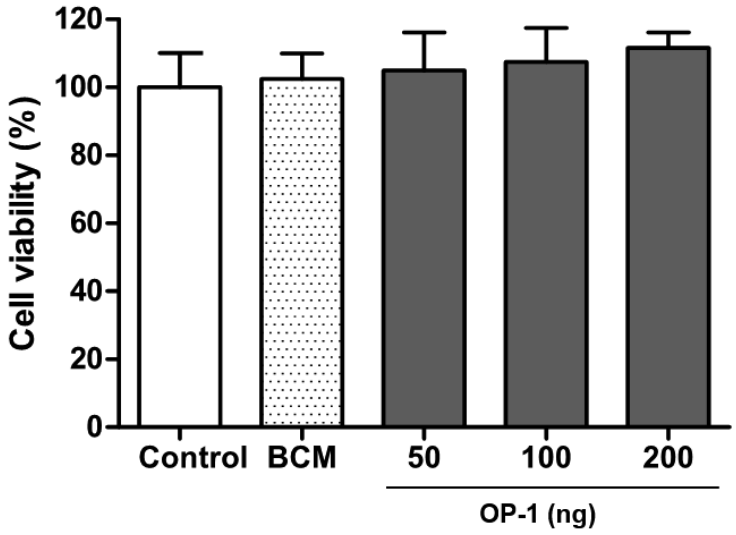

Fig. 3. Cell viability with BCMs containing rhOP-1 (50, 100, or 200 ng) evaluated by MTT assays. The percentage of cell viability was calculated by comparing the appropriate luminescent signal obtained with the control cells. Each value represents the mean ± standard deviation from triplicate samples.

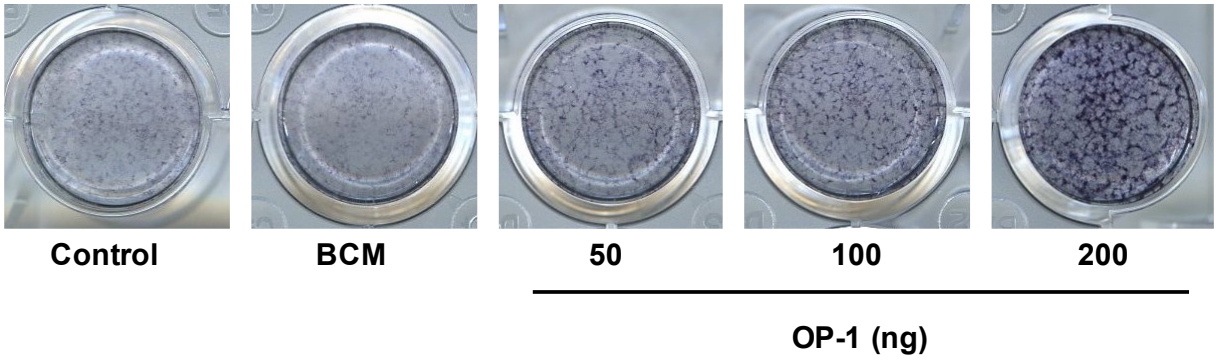

Fig. 4. Osteoblastogenesis with BCMs containing rhOP-1 (50, 100, or 200 ng), as evaluated by ALP staining.

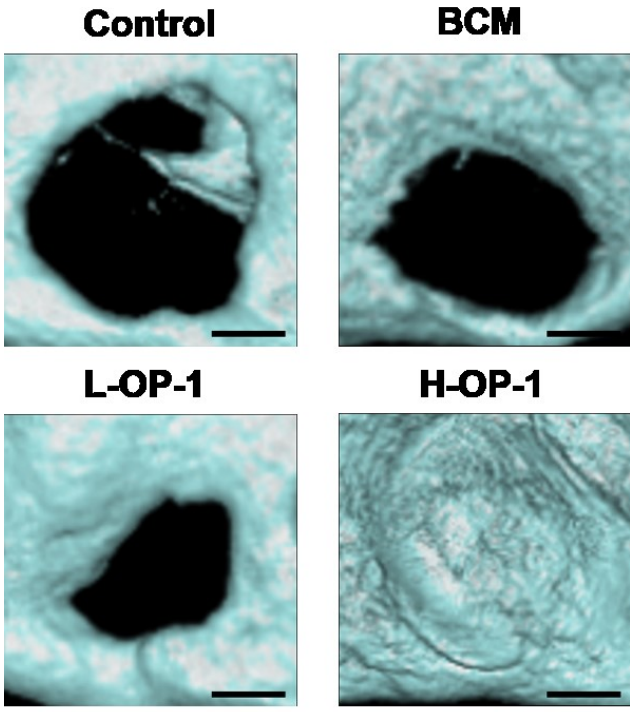

Fig. 5. Representative images of bone formation in rat mandible defects treated with BCM/OP-1 analyzed by micro-CT at 8 weeks after surgery. Four groups were compared: control, BCM alone, BCM containing low-dose (0.5 μg) OP-1 (L-OP-1), and BCM containing high-dose (2.0 μg) OP-1 (H-OP-1). The black color shows nonmineralized defects. Scale bars: 1 mm.

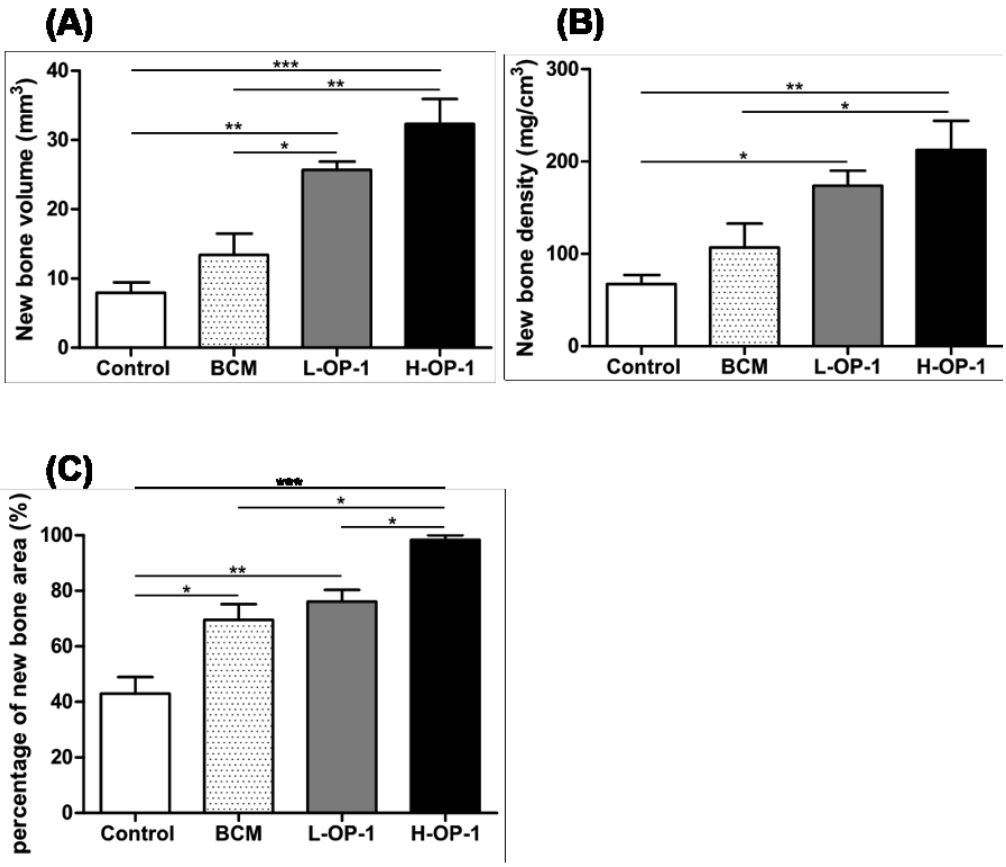

Fig. 6. Quantitative micro-CT analysis of new bone formation: (A) bone volume (mm^3), (B) new bone density (mg/cm^3), and (C) percentage of new bone area (%) in rat mandible defects treated with BCM/OP-1 at 8 weeks after surgery. Four groups were compared: control, BCM alone, L-OP-1, and H-OP-1. *$p < 0.05$, **$p < 0.01$, and ***$p < 0.001$.

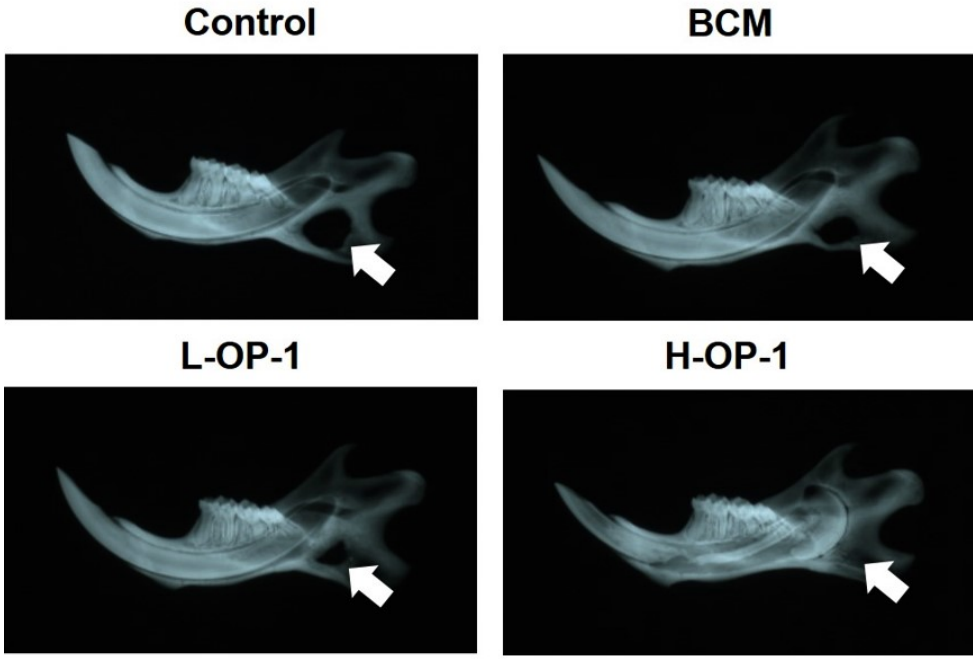

Fig. 7. Representative X-rays of specimens for the different treatment groups at 8 weeks after surgery. Original magnification, 1.0×. White arrow: wounded area.

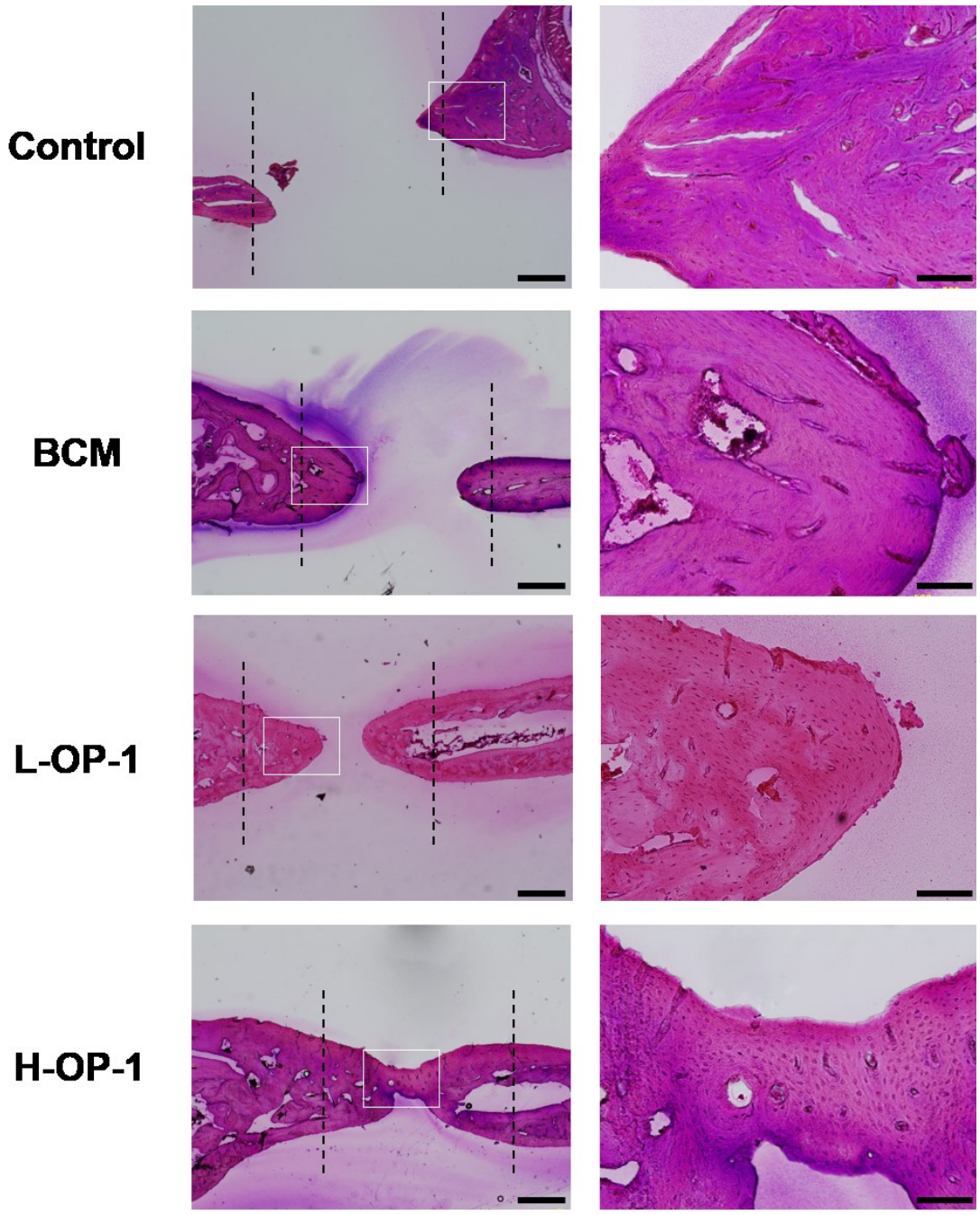

Fig. 8. Histological analysis of newly regenerated bone after application of BCM or BCM/OP-1. Newly regenerated bone in the defects of control (untreated), BCM alone,

L-OP-1, and H-OP-1 groups was evaluated histologically. Hematoxylin and eosin staining of rat mandibular histological sections was performed at 8 weeks after surgery. The dotted lines indicate the edges of the host bone, and the asterisks indicate newly regenerated bone. Scale bars: 1 mm and 250 μm in low- and high-magnification images, respectively.

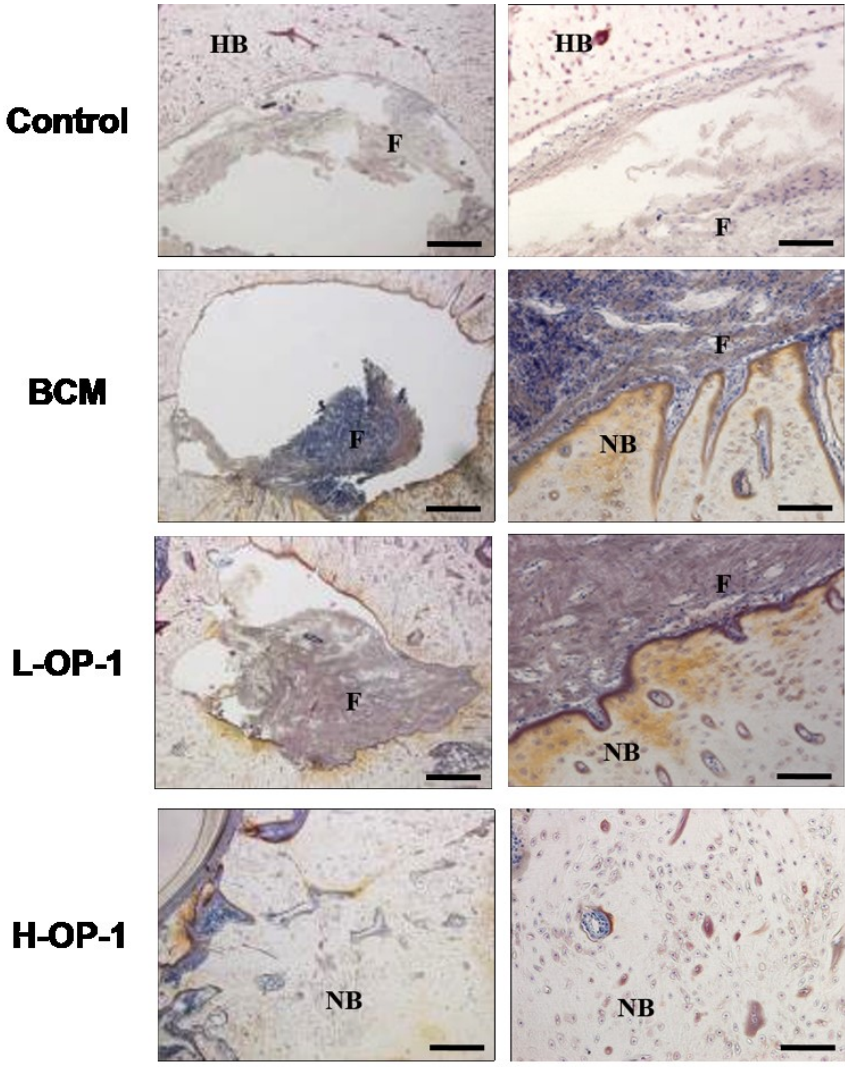

Fig. 9. Light microscopic images (4–20×) showing regenerated bones at 8 weeks after the application of BCM/OP-1 to rat mandibular bone defects. The specimens were stained with Villanueva bone stain solution. Scale bars: 500 and 100 μm in low- and high-magnification images, respectively. HB: host bone, NB: newly formed bone, F: fibrous tissue.

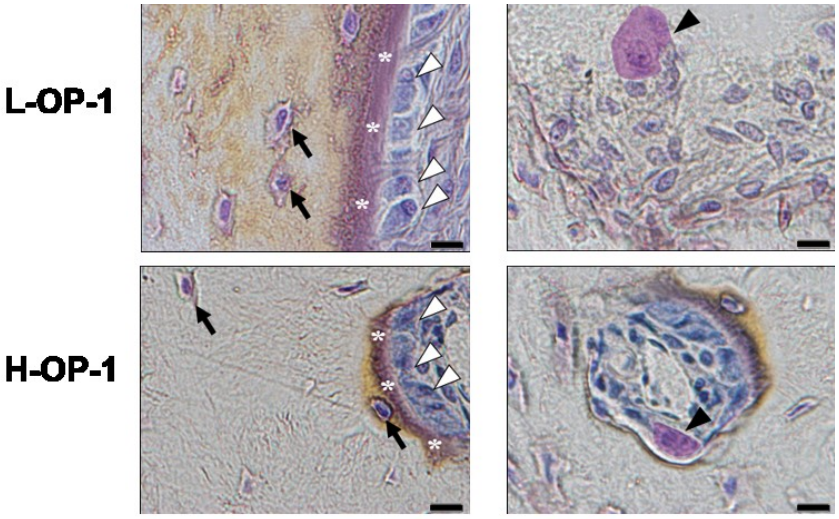

Fig. 10. BCM/OP-1 accelerated the differentiation of osteoblasts and osteoclasts at 8 weeks after surgery in new bone formation. Villanueva bone staining of sections of newly formed bones induced by L-OP-1 (upper panel) or H-OP-1 (lower panel) at 8 weeks after surgery. White arrowheads, black arrows, and asterisks indicate osteoblasts, osteocytes, and osteoids, respectively (left), and black arrowheads show osteoclasts (right). Scale bars: 10 μm.